Original Paper

Thermal Analysis of a Film Cooling System with Normal Injection Holes Using Experimental Data

Kyung Min Kim[1], Dong Hyun Lee[1], Hyung Hee Cho[1] and Moon Young Kim[2]

[1]Department of Mechanical Engineering, Yonsei University
262 Seongsanno, Seodaemun-gu, Seoul, 120-749, Korea
[2]Gas Turbine Technology Service Center, Korea Plant Service & Engineering (KPS)
247 Gyeongseo-dong, Seo-gu, Incheon, 404-170, Korea

Abstract

The present study investigated temperature and thermal stress distributions in a film cooling system with normal injection cooling flow. 3D-numerical simulations using the FEM commercial code ANSYS were conducted to calculate distributions of temperature and thermal stresses. In the simulations, the surface boundary conditions used the surface heat transfer coefficients and adiabatic wall temperature which were converted from the Sherwood numbers and impermeable wall effectiveness obtained from previous mass transfer experiments. As a result, the temperature gradients, in contrast to the adiabatic wall temperature, were generated by conduction between the hot and cold regions in the film cooling system. The gradient magnitudes were about 10~20K in the y-axis (spanwise) direction and about 50~60K in the x-axis (streamwise) direction. The high thermal stresses resulting from this temperature distribution appeared in the side regions of holes. These locations were similar to those of thermal cracks in actual gas turbines. Thus, this thermal analysis can apply to a thermal design of film cooling holes to prevent or reduce thermal stresses.

Keywords: Gas turbine heat transfer, Film cooling, Thermal analysis, Thermal stress, Finite element method

1. Introduction

Film cooling is a method to introduce a coolant fluid into a boundary layer on a surface exposed to a high temperature environment to protect that surface both in the immediate region of injection and in downstream regions as noted by Goldstein [1]. To enhance the performance of film cooling systems, many groups [2-8] have researched the characteristics of fluid flow and heat transfer as well as film cooling effectiveness. By increasing the turbine inlet temperature, the temperature difference between materials increases, which generates high thermal stresses. For example, thermal cracks near film cooling holes have often been observed as shown in Fig. 1, in addition to cracks resulting in system failures as reported by EPRI (Wan et al. [9]). However, most previous studies of hot components have mainly focused on fluid dynamics and heat transfer (or performance) enhancement. To predict the life and safety of hot components such as combustors, vanes, and blades, it is necessary to estimate the metal temperature of the film cooling system in an appropriate thermal environment. In recent years, several investigators [10-12] have attempted a conjugated analysis of heat conduction in turbine blades. In these conjugate analyses, blade surface temperatures and thermal stresses are predicted. It has been shown that the computational results are useful for inspecting the thermal environment of the gas turbine blade and defining the factors that contribute to advanced maintenance and operation. Therefore, the objective of this technical brief is to determine the temperature and thermal stress distributions in a film cooling system with normal injection. Moreover, we conduct thermal analysis using experimental heat transfer data [5-7] as boundary conditions, because the experimental data provide the more accurate boundary conditions, especially near holes having complicate flow pattern.

2. Research Methods

2.1 Conversion of Heat Transfer Data

The heat transfer data around the film cooling system were obtained from previous studies [5-7]. The previous experiments were conducted at a blowing rate (M) of 0.57, with a hole diameter (D_{eff}) of 25.4 mm, hole-to-hole spacing of 3.0 D_{eff}, wall
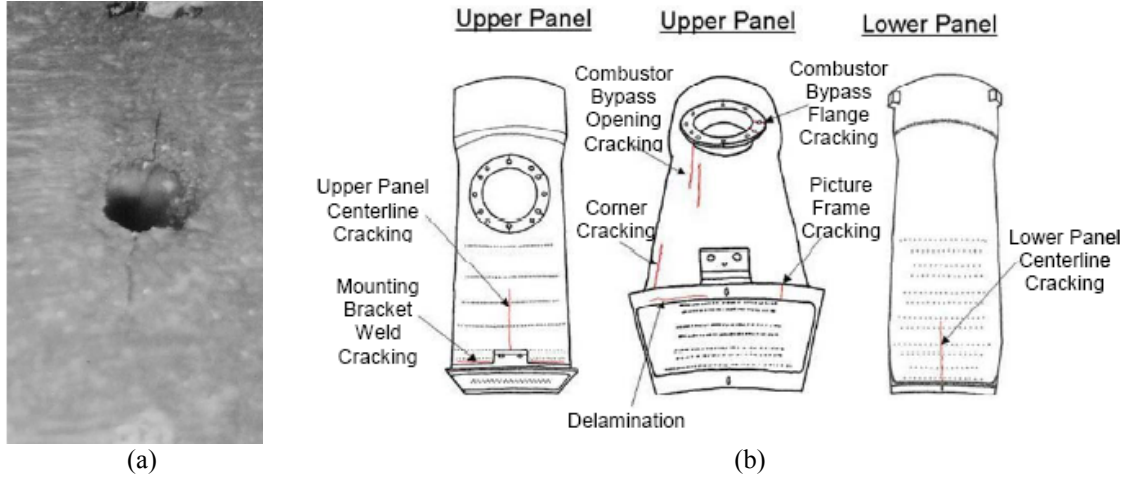
(a)   (b)

Fig. 1 Thermal damage (Wan et al. [9]); (a) cracking at the edge of a film cooling hole, (b) types of cracking observed in service

Table 1 Physical properties of the super-alloy

Temperature [℃]	Thermal Conductivity [W/m-℃]	Thermal Expansion Coefficient [μm/m-℃]	Young's Modulus [GPa]	Poisson's Ratio
100	11.4	11.1	208.8	0.382
300	14.9	13.3	198.6	0.384
500	18.3	14.0	184.6	0.387
700	21.8	14.6	166.9	0.391
900	25.2	15.4	145.5	0.397
1100	28.7	17.3	122.9	0.402

thickness (or jet hole length) of 1.5 D_{eff}, and main flow velocity of 8.8 m/s. The experimental system was larger than an actual film cooling system. Therefore, in the present study, to simulate the actual film cooling system in vanes and combustors, we changed the system geometry and conditions to a blowing rate of 0.57, a hole diameter (D_{eff}) of 4.0 mm, a wall thickness of 1.5D_{eff}, and a main flow velocity of 65.8 m/s to keep the same Reynolds number and blowing rate. Using dimensional analysis (scaling laws), the previous mass transfer data (Sh, η_{iw}) were converted into surface heat transfer coefficients (h) and adiabatic wall temperature (T_{aw}) in the scaled-down system. To calculate the temperature and thermal stresses in the film cooling system, wall temperature (T_w) and wall heat flux (q_w) were calculated from the converted heat transfer data (h, T_{aw}) using the following heat transfer equations:

$$q_w = h(T_w - T_{aw}) \tag{1}$$

$$\eta_{aw} = \frac{T_{aw} - T_\infty}{T_2 - T_\infty} \tag{2}$$

where the operating and material conditions were considered as follows: (1) a coolant flow temperature (T_2) of 700 K; (2) a main hot flow temperature (T_∞) of 1600 K; (3) with the material properties of the super-alloy in Table 1 imposed.

2.2 Thermal Stress Analysis

A stress analysis was conducted to determine the thermal damage of the noted geometries in the film cooling system. The numerical analysis was performed using a commercial code, ANSYS Workbench-11, to calculate the thermal stresses. In numerical calculations, the boundary conditions used the temperature data calculated from eqs. (1) and (2).

To calculate the thermal stresses, constraints with uniform deformation in the x-axis direction due to the existence of additional materials and symmetric conditions were imposed as shown in Fig. 2. Because most stresses are caused by settlements of constraints and thermal effects (arising from temperature changes and differences), constraints are important. Furthermore, the thermal stress for structural materials is proportional to the temperature change (α) and temperature difference (ΔT) as noted in Equation (3):
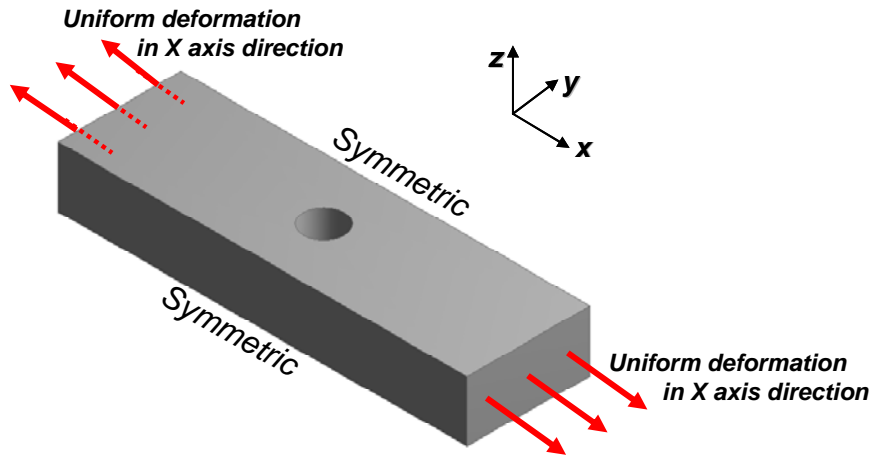
$$\sigma = E\alpha(\Delta T) \tag{3}$$

Fig. 2 Geometry and boundary conditions of the film cooling system

(a) Adiabatic wall temperature on the exposed surface

(b) Heat transfer coefficients on the exposed surface

(c) Heat transfer coefficients on the back surface

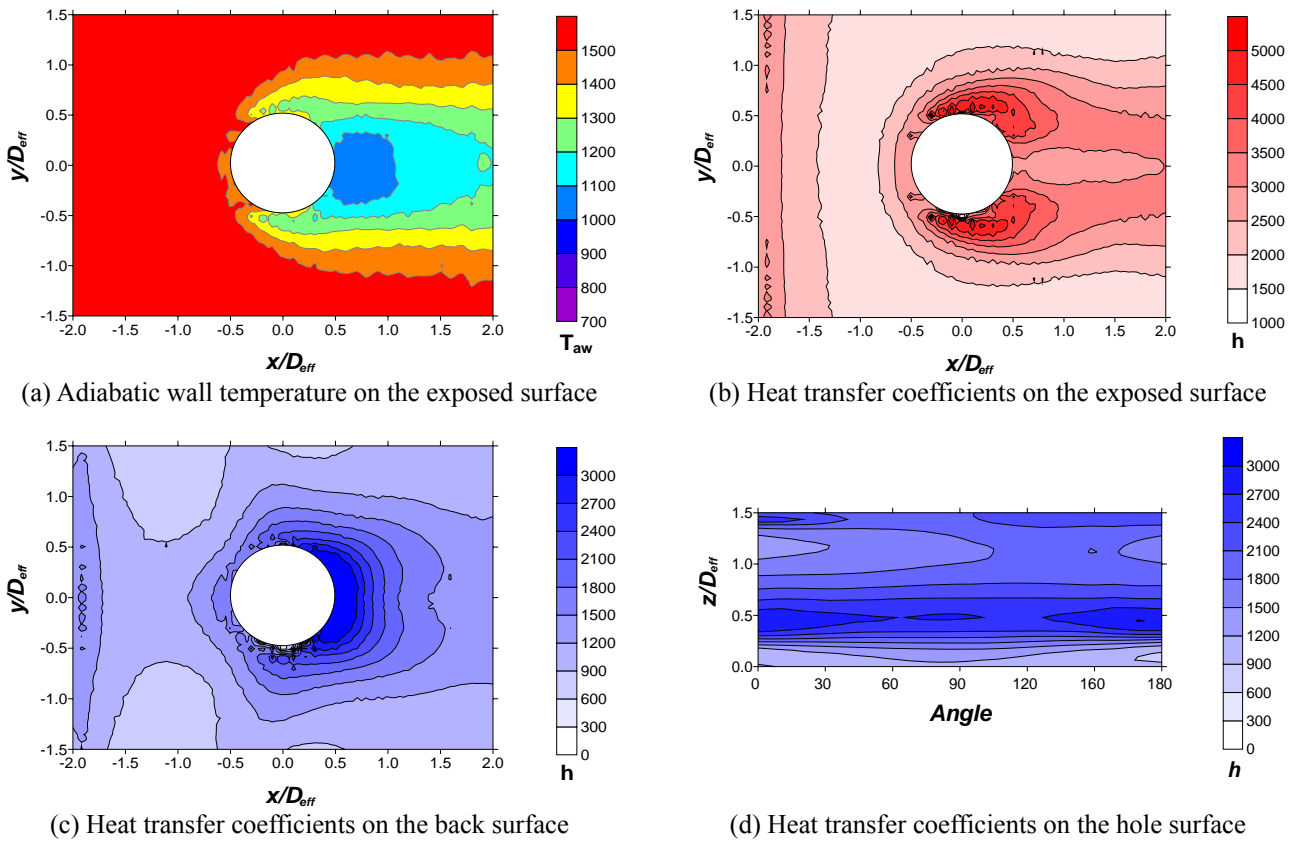(d) Heat transfer coefficients on the hole surface

Fig. 3 Converted data for thermal analysis

In the calculated results, the equivalent or von-Mises stress (σ_v) is used because it is a part of the maximum stress failure theory used to predict yielding in a ductile material. The finite element thermal analysis in the present work was conducted as follows: (1) Create a test model using the finite elements; (2) Define boundary conditions and the material properties; (3) Calculate the temperature distributions by conduction in the 3D test model; (4) Calculate the thermal stresses using the temperature distributions and constraint conditions.

3. Results and Discussion

3.1 Converted Heat Transfer Distributions

Figure 3 shows heat transfer distributions that convert the previous film cooling data obtained by Cho and Goldstein [5-7] into suitable data at D_{eff}=4.0 mm in the present case. The characteristics of the heat transfer distributions are reviewed briefly based on the studies of Cho and Goldstein [5-7]. In view of the thermal design for film cooling, the correct analysis of overall heat transfer
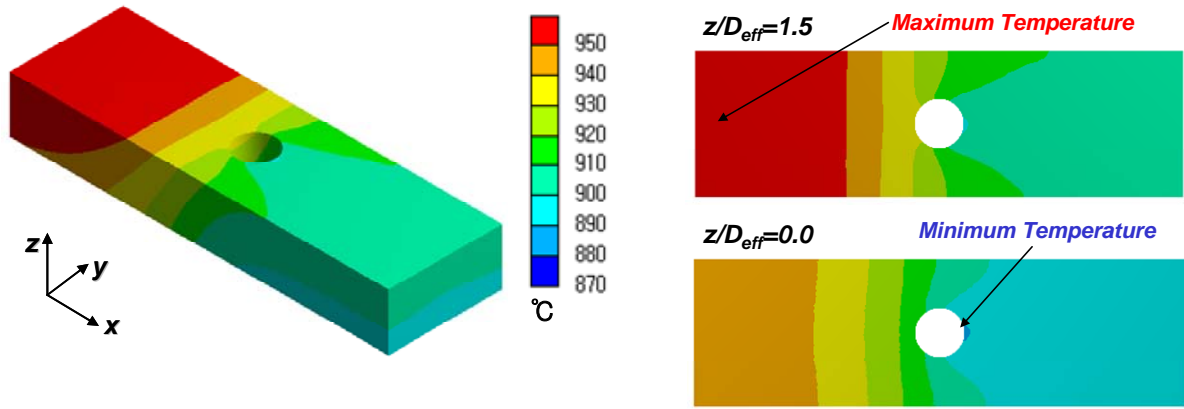
(a) Temperature distributions
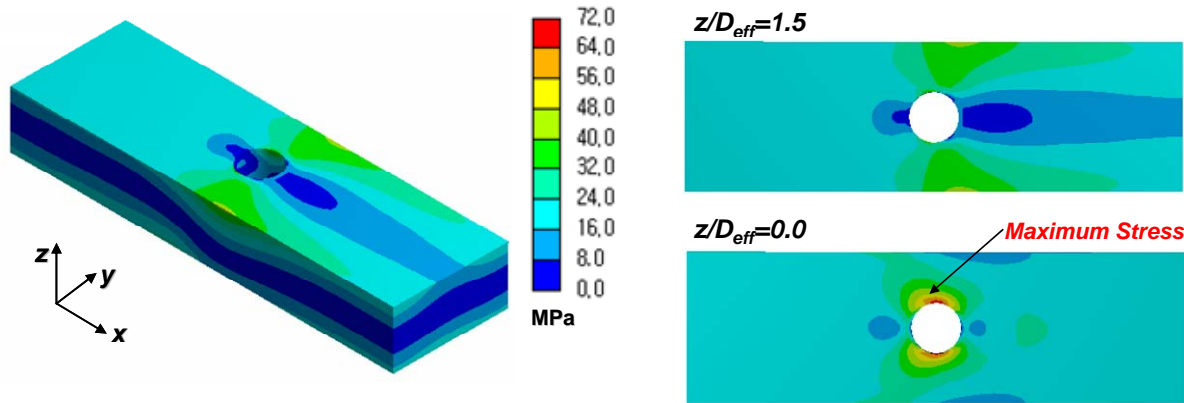
(b) Thermal stress distributions

Fig. 4 Results of thermal analysis in the film cooling system

requires four sets of data: the adiabatic wall temperature (film cooling effectiveness), the heat transfer coefficient distribution on exposed surfaces, the heat transfer coefficient distribution on internal surfaces, and the heat transfer coefficient on surfaces inside the hole.

First, the pattern of adiabatic wall temperature (Fig. 3(a)) can be explained by the mixing of the jet stream from the down-washing vortex of the cross-flow and/or by the vortex shedding of the jet stream. The adiabatic wall temperature obtains a minimum value at the edge of the injection hole and increases downstream from the hole.

Second, in this region, the characteristics of heat transfer coefficient distributions (Fig. 3(b)) can be divided into three different regions: (1) in the region upstream of the injection hole, heat transfer is only slightly changed due to jet injection. That is, the heat transfer rate is slightly increased; (2) in adjacent side regions of the injection hole, the heat transfer is greatly increased because of the interaction of the main flow and the injected jet. The side vortex, created by shearing action, is formed near the surface where the injected jet stream spreads on the surface by the main flow. The side vortex is responsible for the high transfer coefficients; (3) in the region downstream of the injection hole, the low heat transfer region is bounded because the strength of the side vortices is diminished.

Third, local values of the heat transfer coefficient on the back surface of the hole entrance are shown in Fig. 3(c). On the back surface near the effusion holes, the heat transfer coefficients were higher than those in other regions because the tripping flow effected a stronger reattachment around the holes. It is noted that the tripping flow near the back surface is entrained into the effusion (film cooling) holes, and then spent air, which is not expelled through the hole, collides with the region behind the hole.

Lastly, the angle around the inside of the hole is measured from the leading edge (0 deg.) of the injection hole to the trailing edge (180 deg.) with respect to the mainstream flow as shown in Fig. 3(d). According to the flow pattern, the heat transfer characteristics inside the hole can be divided into four different regions: (1) in the separation/recirculation region, the heat transfer is usually low due to recirculation of the flow; (2) in the reattachment region, a high heat transfer appears because the flow is interrupted by the wall; (3) in the developing region, after reattachment, the boundary layers of flow and heat transfer develop and the heat transfer slowly decreases. In this region, heat transfer is affected weakly by the main hot gas flow at the exit; (4) in the region near the exit of hole, heat transfer is directly affected by this main flow.

3.2 Temperature and Thermal Stresses

Figure 4 shows the temperature and thermal stress distributions in the film cooling system. The figures consist of the overall 3D-distribution, exposed surface (z/D_{eff}=1.5), and back surface (z/D_{eff}=0.0). As shown in Fig. 4(a), the overall distributions suggest that the temperature is high in the upstream region, and becomes lower downstream. In contrast to the local adiabatic wall
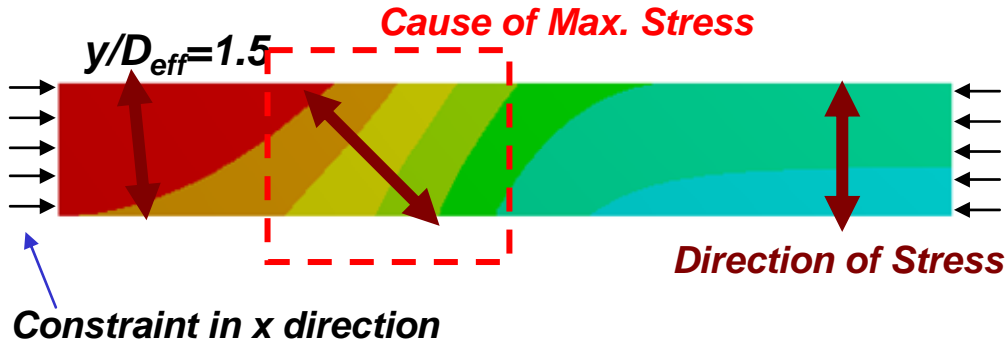
Fig. 5 Cause of the high thermal stress

temperature distributions in Fig. 3(a), the temperature gradients in the x- and y-axis directions are generated by conduction between the hot gas section and cold section. Furthermore, the temperature gradient in the side regions of the cooling hole becomes steeper than other regions due to the high heat transfer rate and the clear difference of adiabatic wall temperature on the exposed surface (z/D_{eff}=1.5) as shown in Fig. 3(b). The gradient magnitudes in x- and y-axis directions are about 50-60 K and 10-20 K, respectively. Also, the maximum and minimum temperatures in the overall material are 968.9℃ and 889.2℃, respectively.

The thermal stresses resulting from these temperature distributions are presented in Fig. 4(b). High thermal stress distributions appear in the side regions of the hole. The reason for this finding is as follows: (1) as shown in Fig. 5, the temperature gradient in upstream and downstream regions appears in the same direction relative to the y-axis, but in the middle region (red-dash line box) has constraints in the x-axis direction. That is, because the direction of thermal expansion and stress are the same as the temperature gradient direction in eq. (3), the high thermal stresses are contained in the middle region; (2) the maximum stress occurs in the adjacent side of the hole on the back surface (z/D_{eff}=0.0). The magnitude of this stress is 75.56 MPa, which results from the differences in thermal expansion between the upstream region and downstream region. In other words, because the thermal expansion in the upstream region is larger than that in the downstream region, the thermal stresses are more concentrated in the low temperature section of the middle region. These stresses cause thermal cracks in the side regions as mentioned in Fig. 1.

4. Conclusions

The present study investigated the thermal characteristics of film cooling with 90 deg. injection holes using experimental local heat transfer and film cooling effectiveness data. The boundary conditions used converted data, namely heat transfer and adiabatic wall temperature data. Numerical simulations using ANSYS Workbench-11 commercial code were conducted to calculate the distributions of temperature and thermal stresses based on local experimental data.

The calculated temperature in the film cooling system was high in the region upstream of the cooling hole on the exposed surface, but decreased in the region downstream of the cooling hole on the exposed surface and in the overall region of the back surface. Temperature gradients in the film cooling system were generated by conduction between these hot and cold regions. The gradient magnitudes were about 10-20K in the y-axis direction and about 50-60K in the x-axis direction. High thermal stresses appeared around the holes. This is because the temperature difference before and after the cooling hole is large and steep in the x-axis direction. Furthermore, this direction included constraints from additional materials. In summary, thermal analysis using local experimental data is suitable for predicting accurate thermal damage. To reduce the large and dramatic temperature difference (thermal stress) between various hot components, further studies on thermal design, including both thermal analysis and heat transfer control, are required.

Nomenclature

D_{eff}	hole diameter	T_w	wall temperature
E	Young's modulus	T_∞	main flow temperature
h	heat transfer coefficients	q_w	wall heat flux, eqn. (1)
M	blowing rate	α	thermal expansion coefficient
Sh	Sherwood number (non-dimensional mass transfer coefficient)	η_{aw}	adiabatic wall cooling effectiveness, eqn. (2)
		η_{iw}	impermeable wall effectiveness, $\eta_{iw} = \eta_{aw}$
T_2	secondary (coolant) flow temperature	σ_v	von Mises stress
T_{aw}	adiabatic wall temperature		

References

[1] Goldstein, R. J., 1971, "Film Cooling," Advances in Heat Transfer, Vol. 7, pp. 321-379.
[2] Goldstein, R. J., Eckert, E. R. G., and Burggraf, f., 1974, "Effects of Hole Geometry and Density on Three-Dimensional Film

Cooling," Int. J. of Heat Mass Transfer, Vol. 17, pp. 595-607.

[3] Leylek, J. H. and Zerkle, R. D., 1994, "Discrete-jet Film Cooling: A Comparison of Computational Results with Experiments," ASME J. of Turbomacinery, Vol. 116, No. 3, pp. 321-379.

[4] Schmidt, D. L., Sen, B., and Bogard D. G., 1994, "Film Cooling With Compound Angle Holes: Adiabatic Effectiveness," ASME J. of Turbomacinery, Vol. 118, No. 4, pp. 807-813.

[5] Cho, H. H. and Goldstein, R. J., 1995, "Heat (Mass) Transfer and Film Cooling Effectiveness With Injection Through Discrete Holes: Part I-Within Holes and on the Back Surface," ASME J. of Turbomachinery, Vol. 117, No. 3, pp. 440-450.

[6] Cho, H. H. and Goldstein, R. J., 1995, "Heat (Mass) Transfer and Film Cooling Effectiveness With Injection Through Discrete Holes: Part II-On the Exposed Surface," ASME J. of Turbomachinery, Vol. 117, No. 3, pp. 451-460.

[7] Goldstein, R. J., Cho, H. H., and Jabbari, M. Y., 1997, "Effect of Plenum Crossflow on Heat (Mass) Transfer Near and Within the Entrance of Film Cooling Holes," ASME J. of Turbomachinery, Vol. 119, No. 4, pp. 761-769.

[8] Cho H. H., Kang, S. G., and Rhee, D. H., 2001, "Heat/Mass Transfer Measurement Within a Film Cooling Hole of Square and Rectangular Cross Section," ASME J. of Turbomacinery, Vol. 123, No. 4, pp. 806-814.

[9] Wan, E., Hong, C., Dewey, R., Bernstein, H., and Norsworthy, D., 2005, "Life Management System for Advanced F Class Gas Turbine," EPRI Report 1008319.

[10] Geidmann, J. D., Kassab, A. J., Divo, E. A, Rodriguez, F., and Steinthorsson, E., 2003, "Conjugate Heat Transfer Effects on a Realistic Film-Cooled Turbine Vane," ASME Turbo Expo 2003, Atlanta, USA, Paper No. GT2003-38553.

[11] Nowak, G. and Wroblewski, W., 2007, "Thermo-mechanical Optimization of Cooled Turbine Vane," ASME Turbo Expo 2007, Montreal, Canada, Paper No. GT2007-28196.

[12] Tinga, T., Kampen, J. F., Jager, B, and Kok, J. B. W., 2007, "Gas Turbine Combustor Liner Life Assessment Using a Combined Fluid/Structural Approach," ASME J. of Eng. for Gas Turbines and Power, Vol. 129, No. 1, pp. 69-79.